

# Ventilation and pollutant dispersion in a group of courtyard buildings with a diagonal wind

Simone Ferrari<sup>1\*</sup> and Luca Tendas<sup>1</sup>

<sup>1</sup> DICAAR - Dipartimento di Ingegneria Civile, Ambientale e Architettura, University of Cagliari, via Marengo 2, 09123 Cagliari, Italy

**Abstract.** The urban built environment strongly modifies the wind flows and, consequently, can cause heat and pollutant accumulation. The former contributes to generate the Urban Heat Island phenomenon, the latter to the increase in health issues recorded in the cities. Both of them can be mitigated through the proper implementation of the Urban Microclimate Design, which is a design and planning strategy employing the shape and layout of buildings to optimize comfort, air quality and energy efficiency of the built environment and, consequently, contributing to the generation of mitigative cities. In this paper, we present a parametric study, via numerical simulations employing the ENVI-met<sup>®</sup> three-dimensional microclimate model, of the ventilation and of the dispersion of a pollutant inside and outside a group of courtyard buildings hit by a diagonal wind. All the variables are kept constant, except the length of the internal courtyard, which is the variable parameter. The results suggest that the shape of these buildings biases the air flows and pollutant behaviour, so pointing out that it can be efficiently used to improve the air quality and the outdoor human comfort in the modern cities.

## 1 Introduction

A courtyard building is a construction with an inner unroofed open space surrounded by the walls of the building itself. As exposed by Sharples and Bensalem, 2001 [1], the courtyard buildings have faced a renewed interest in both residential and non-residential constructions, thanks to their capability to provide an internal outdoor environment with mitigated conditions in relations to the external ones, for both thermal comfort and air quality. At the same time, that internal space offers more privacy and quietness than other outdoor spaces (Gidlöf-Gunnarsson and Öhrström, 2010 [2]). Moreover, the courtyard building, when properly dimensioned and shaped, can make use of natural ventilation, for both external and internal spaces, so reducing the energy consumption of the whole building (Ok et al., 2008 [3]).

The courtyard building has a long history, starting from ancient Greece and Rome and arriving, through the traditional Arab architecture, till the mid of the 20<sup>th</sup> century, when it found a period of decline, due to the reduced necessities of building natural cooling and warming caused by the possibility to mechanically mitigate the interior temperature.

Nowadays, the growing costs of energy, as well as the necessity to reduce pollutant emissions, have generated the above stated renewed interest in this kind of building: for instance, most of the large commercial buildings erected during the last 40 years are in the form of courtyards, frequently with an open central core intended for circulation and resting purposes. In

addition, as stated, among the others, by Ratti et al., 2003 [4], the courtyard building is the building form that makes the better use of land in environmental and microclimate terms, in particular (but not only) for the urban environments in hot arid climates. An extensive review on the microclimatic capabilities of courtyards can be found in Zamani et al., 2018 [5].

The Urban Microclimate Design can be defined as a multidisciplinary process aiming at optimizing the outdoor human comfort in the urban built environment, in a sort of circular process taking into account the (sometimes conflicting) instances of architectural and microclimatic point of view (Chiri et al., 2020 [6]). As a matter of fact, several studies (see e.g. Santamouris, 2001 [7] and De Pascali, 2008 [8]) have demonstrated that a design approach based on the comfort and energy optimization of a single building without taking into account its position in the surrounding built environment will lead to a reduction of its performances. For this reason, in many States (e.g., United Kingdom and China) a quantification of the outdoor comfort in the built environment is compulsory in the design of new buildings, while in many others it is recommended (Eliasson, 2000 [9]).

Moreover, as reported by the United Nations' World Health Organization (WHO, 2021, [10]), most of the world population suffers a rise of diseases and fatalities due to the explosion of urban pollution. As a matter of fact, as demonstrated, among the others, by Kurppa et al., 2018 [11], Badas et al., 2018 [12], and Ferrari et al., 2019 [13], the urban environment causes accumulation of pollutant between buildings.

\* Corresponding author: [ferraris@unica.it](mailto:ferraris@unica.it)

As a consequence, the targets of the contemporary urban design and planning are the optimization of human outdoor comfort and air quality, as well as the reduction of the pollutant accumulation: the main driver for reaching these targets is the proper modelling of ventilation (i.e., the wind velocity and the consequent air exchange between the urban environment and the external atmosphere, Tamura, 2016 [14]) through geometrical strategies, the most efficient, according to the review of Lai et al, 2019 [15].

This can be achieved through a site-specific design based on parametric studies: in fact, if the former (site-specific design) is essential, due to the complexity of urban environment, but yields non-generalizable results, the latter (parametric study) is crucial when deciding which building parameters (e.g., height to width ratio of buildings and street canyons) employ in the peculiar case.

Moreover, both the design approaches can be undertaken via laboratory or numerical simulations (a review of the techniques to investigate the turbulent air flows involved can be found in Ferrari et al., 2022 [16]). For instance, Di Bernardino et al., 2017 [17] investigated in the laboratory, the effect of the different positions of a pollutant source on a single isolated building (via a Laser Induced Fluorescence technique, see, e.g., Ferrari and Querzoli, 2015 [18], for a description), while Ferrari et al., 2017 [19], Garau et al., 2018 [20], and Badas et al., 2020 [21], experimentally measured velocity and turbulent quantity fields through image analysis techniques (see Ferrari, 2017 [22], for a review). On the numerical simulations side, Badas et al, 2017 [23], Garau et al., 2019 [24], Sun et al., 2021 [25] and Cui et al., 2021 [26], simulated different building configurations where the influence of the variation of a single geometrical parameter on the ventilation in the urban environment was investigated. Moreover, it is now possible to extract, via non-supervised codes relying on free online available Geographic Information System (GIS) databases (Badas et al., 2019 [27] and Salvadori et al., 2021-a [28]), the values of the geometrical parameters of the urban texture in real cities, increasing the possibilities to describe the influence of the urban canopy on the atmospheric flows and to create maps of the potentialities of the cities for various scopes, as, for example, for small scale wind turbine location (Salvadori et al., 2021-b [29]).

Regarding the site-specific investigation on courtyards, Ernest and Ford, 2012 [30], have performed a in-field measurement campaign in Seville (Spain), finding out that courtyards in semi-arid climates promote convective cooling and, consequently, improve the local microclimate. Xu et al., 2018 [31], have numerically evaluate the performance of the traditional courtyard design in China, finding that a proper modulation of the courtyard aspect ratio (AR, i.e. the ratio of the inner courtyard length to the courtyard height) improves the natural ventilation. Rodríguez-Algeciras et al., 2018 [32], carried out both a parametric and site-specific analysis on the temperature and outdoor comfort of square and rectangular courtyards with different orientation, but without taking into account the ventilation effects or the presence of groups

of courtyards. Rivera-Gómez et al., 2019 [33], performed an extensive in-field measurement campaign on the courtyard mitigation potential in Spain, finding that, in all the case investigated, the outdoor temperature decreases down to 3–15 °C. Ma et al., 2019 [34], performed numerical simulations on the pollutant dispersion in various typologies of courtyards and clusters of courtyards found in typical Chinese urban environments. Piedra et al., 2020 [35], performed numerical and laboratory simulations (on a single courtyard building with different dimensions and orientations to the wind), as well as in-situ measurement campaign, demonstrating the positive impact of courtyards for reaching ventilation and natural lighting standards. Diz-Mellado et al., 2021 [36], evaluated in-site the thermal comfort in two courtyards, with different AR, in Cordoba (Spain). Du et al., 2022 [37], carried on a site-specific investigation on Chinese courtyards and on how different architectural aspects can improve or decrease natural ventilation. Callejas and Krüger, 2022 [38], evaluated the natural ventilation properties of historic courtyard buildings in tropical climate, through in-field measurement campaigns and surveys with the visitors of the buildings, finding out that, depending on the geometrical features, courtyard buildings can promote natural ventilation.

Regarding the parametric investigations on courtyards, Sharples and Bensalem, 2001 [1], experimentally studied in the wind tunnel several configurations of single courtyards, both with perpendicular and inclined wind, but not group of courtyards. Taleghani et al., 2014 [39], investigated, via numerical simulations with the ENVI-met® software validated through field data, the ventilation on courtyards with different size and with diagonal wind, but not groups of courtyards. Martinelli and Matzarakis, 2017 [40], carried out a theoretical investigation of the influence on the Sky View Factor (SVF) and on the outdoor human comfort of the courtyard AR in the Italian climate. Ying et al., 2020 [41] studied different openings in the courtyard buildings and their influence on ventilation. Callejas et al., 2020 [42], investigated the impact of AR the thermal conditions in a single courtyard. Ferrari, 2022-a [43] and 2022-b [44], studied numerically the effect of the variation of the parallel-to-the-wind size of the internal courtyard respectively on the ventilation and pollutant dispersion in a group of courtyards hit by a perpendicular wind.

As it can be noticed from the above shown literature review and to the best of the authors' knowledge, a parametric study on the effect of a different value of the internal courtyard size on the ventilation and pollutant dispersion of a group of courtyards buildings, hit by a diagonal wind, has not been performed, thus far. As a consequence, and to integrate the last two cited works, the target of this work is to investigate the effect of the variation of one of the size of the internal courtyard on the ventilation and pollutant dispersion inside and outside a group of courtyard buildings, hit by a diagonal wind, through numerical simulation using the microclimate model ENVI-met® (Bruse and Fleer, 1998 [45], see the next Section for a short description of this model).

In the following, this paper is organized in this way: in Section 2, the details of the group of courtyards and of the simulation parameters will be given, in Section 3 the main results about ventilation and pollutant dispersion will be shown and discussed, and eventually in Section 4 the main conclusions will be drawn.

## 2 Materials and methods

Fig. 1 shows the investigated group of four identical courtyards, with flat roof, where the building height (10m), thickness (10m) and internal width  $W$  (5m) are kept constant, as well as the distances among courtyards (or, from another point of view, the street width; 10m), while the internal length  $L$  is the variable parameter (5m, 10m, 15m, 20m). As a consequence, the simulated configurations will be identified as W5L05, W5L10, W5L15 and W5L20. On Fig. 1 the names of the courtyards (abbreviated, in the following, in C.1, C.2, C.3 and C.4) and of the streets (abbreviated, in the following, in S.1, S.2 and S.3) are reported. The building dimensions have been chosen as typical of some residential configurations in small and medium Italian villages.

A constant wind, coming from the East-South-East direction (angle of  $120^\circ$  from the North) and with an undisturbed velocity  $U_0$  of 1.15 m/s, temperature ( $19.8^\circ\text{C}$ ) and meteorological parameters were employed in all the simulations: these values are the mean ones measured from the meteorological station of Rome-Ciampino (Italy) on the 23 June 2018, the day chosen for the simulations (the summer solstice).

A whole day (24 hours) was simulated, starting from the 6am. A source of carbon monoxide CO (simulating a chimneystack) was placed 2m on the roof of C.1: the flow rate and the concentration  $C_0$  emitted from this source was kept constant.

As one of the targets of the present work is to study the pollutant dispersion, the related results will be shown as concentration reduction  $C_0/C$  and not as actual concentration values.

The computational domain was chosen, according to Blocken, 2015 [46], in order to left enough space around the simulated built environment for the flow to reattach after the flow detachment due to the interaction with the obstacles and, consequently, to avoid numerical instability issues. The resolution (the cubical cell size) was 1m, with the first cell close to the ground split into five smaller cells, to have a higher resolution where the logarithmic wind profile, typical of the urban boundary layer, has the highest curvature.

As previously stated, the employed software was ENVI-met<sup>®</sup>, a holistic three-dimensional non-hydrostatic microclimate modelling system widely employed and validated for urban microclimate applications in a specific geographical location. The ENVI-met<sup>®</sup> code is able to simulate the interactions between surfaces, plants and air in the built environment, using the RANS (Reynolds-Averaged Navier–Stokes) equations to compute the air flows, their turbulence and the heat transfer (see, e.g., Mosteiro-Romero et al., 2020 [47]).

The typical spatial resolution of resolution of ENVI-met<sup>®</sup> ranges from 0.5m to 10m, while its typical temporal resolution ranges from 1s to 5s.

ENVI-met<sup>®</sup> is based on four models, namely the atmospheric, soil, vegetation and building models. The first one (the atmospheric model) has the role to calculate the mean air flows, their turbulence, the fluxes of direct, diffuse and reflected short-wave and long-wave radiation, and the air temperature and humidity. The second one (the soil model) has the role of calculating the surface and soil temperatures, and the soil water fluxes. The soil model is strictly coupled to the vegetation model, which has the role to compute the evaporation rates, the foliage temperatures and the fluxes of heat, evaporation and transpiration between the vegetation and the environment. Finally, the fourth model (the building one) has the role of calculating momentum, heat and vapor fluxes linked to the building walls and roofs, depending on the employed material properties.

A typical ENVI-met<sup>®</sup> simulation starts from a set of files, namely the Area Input, Database, and Configuration files. The first one contains the three-dimensional model of the built environment to simulate: often, the information about the terrain elevation can be found as DTM (Digital Terrain Model). The second one (the Database files) contains the information about the materials of the built environment (e.g., soil, vegetation and surface materials, etc.) and of the pollutants, as well as their main characteristics (e.g., thermal conductivity, albedo, water content, type of contaminant, etc.), which can be chosen from the existing databases, included in the software, or user-defined. In the third one (the Configuration file), the settings about the time duration, the weather conditions, the geographical location, the turbulence model to employ, etc. are stored. As a consequence, it is possible to state that ENVI-met includes the main variables and processes involved in urban microclimate evolution, as well as the possibility to simulate the daily variations in sun position and its influence on shading/insulation, useful, for instance, in the comparison of the human outdoor comfort of a new building against then existing situation (see, e.g. Chiri et al., 2020 [6]).

Among the others, Salata et al., 2016 [48], compared the in-field measured data in Rome (Italy) with the ones simulated by ENVI-met<sup>®</sup>, finding a good predictive ability of the software. Forouzandeh, 2018 [49], validated ENVI-met<sup>®</sup> for predicting the microclimate variables inside medium-narrow courtyards, comparing the numerical simulation results with field data and finding an acceptable accuracy. The same author, in 2021 [50], evaluated the accuracy of ENVI-met<sup>®</sup> to simulate the surface temperature of a building in Hanover (Germany), find a good reliability in common urban areas. Sun et al., 2021 [51], Viecco et al., 2021 [52], Wu et al., 2021 [53], and Jing and Liang, 2021 [54], performed various simulations of the pollutant dispersion in different urban configurations with ENVI-met<sup>®</sup>. Karimian Shamsabadi et al., 2022 [55], as well as Kandelan et al., 2022 [56], used ENVI-met<sup>®</sup> for the simulation of the PM<sub>2.5</sub> dispersion in various configurations of building typologies, finding a high

accuracy. Peng et al., 2023 [57], validated ENVI-met<sup>®</sup> on 107 courtyards located in Cambridge (UK) through in-field measurements, finding good agreement. For this reason, as highlighted by Fabbri and Costanzo, 2020 [58], ENVI-met<sup>®</sup> is the most employed software to simulate and support the modelling of the urban outdoor microclimate. Therefore, despite the limitations due to the spatial and temporal discretization in the simulated built environment, and to the approximations introduced by the RANS equations, ENVI-met<sup>®</sup> can be employed as valuable tool for the urban microclimate design, in order to improve, among the others, its energy and microclimatic performance.

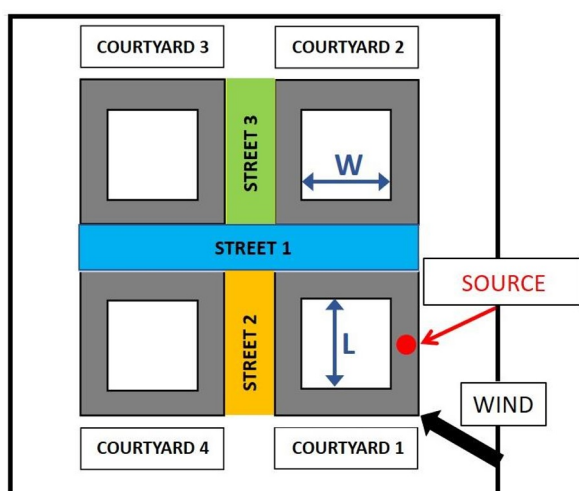


**Fig. 1.** Sketch of the group of courtyards, with the relevant dimensions, the wind direction, the position of the pollutant source, the names identifying the courtyards and the streets.

### 3 Results

In this section, the main results related to the wind velocity values and directions (Subsection 3.1) and the pollutant concentration reductions (Subsection 3.2) will be shown. It is worthwhile stating that the outputs from the numerical simulations are in the form of three-dimensional matrices for each variable and for each hour of the simulated day, so in the following they will be shown in the form of variable field at a fixed position and time, or in the form of variable value versus time at a fixed location.

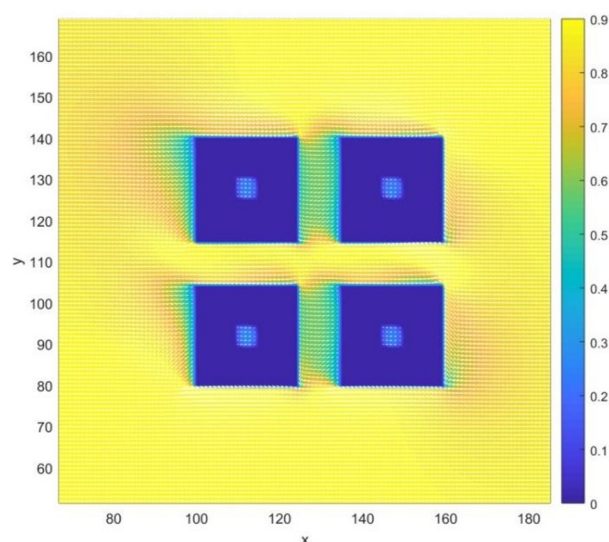
#### 3.1 Wind velocity

Fig. 2 shows a zoom on the group of courtyards of the horizontal field (measured at the buildings' roof level) of the wind velocity magnitude  $U$  in m/s; the velocity values are showed in false colours, so that values close to the maximum are in pale yellow and values close to the minimum (zero) are in dark blue. Moreover, the white arrows represent the velocity direction and magnitude.

As the wind comes from the East-South-East direction, it is visible the different shelter effect of the streets and of the internal courtyards: street 2 and 3 are

protected from the wind, street 1 experiences the highest values of velocity, and in all the internal courtyards the ventilation is reduced.

The effect of the courtyard dimensions on the velocity reduction, that the designer or the urban planner could prefer to enhance or reduce according to desired outdoor comfort and planned scope of the urban environment, will be shown on Fig. from 3 to 7. Moreover, on Fig. 2 the recirculation zones and the wake behind the buildings are visible.



**Fig. 2.** Horizontal field (colour map) of velocity magnitude  $U$  [m/s] at the roof level (the undisturbed velocity  $U_0$  is 1.15 m/s from East-South-East), with the velocity vectors in white, for the configuration W5L05.

As above stated, with the target to quantify the influence of the group of four courtyards and of their internal dimensions in modifying the wind velocity in the inner courtyards, on Fig. from 3 to 6 (for, respectively, the courtyards from C.1 to C.4) the daily variation of the maximum velocity  $U_{MAX}$ , nondimensionalised with the undisturbed wind velocity  $U_0$  and measured in the whole volume of the inner courtyards, is plotted for the four simulated configurations. The values for the case W5L05 are shown by a continuous black line with black circles, for the case W5L10 by a dashed blue line with blue plus signs, for the case W5L15 by a continuous red line with red asterisks and for the case W5L20 by a dashed green line with green circles.

In all the cases, the velocity value in the internal courtyard is proportional to its volume, so the designer should increase the internal courtyard dimensions to increase the ventilation and vice-versa. It is also interesting to note that the first courtyard encountered by the wind, C.1, is also the one that experiences the highest wind velocity reduction, while the C.2 is the one with the highest ventilation, with C.3 and C.4 showing similar values. That can be explained with the different velocity directions, as in the case of the upstream courtyards the velocity at the building top is almost vertical, due to the flow separation, and so has more difficulty in entering the internal courtyard, in the other cases it is almost horizontal, resembling the case of

skimming flow described in Oke, 1988 [59], so it is easier to enter the internal volume of the courtyard.

On Figure 7, the daily variation of the nondimensional minimum velocity  $U_{min}/U_0$  inside the C.1 is shown (the values in the other courtyards are not shown, as they result very similar to the C.1 ones).

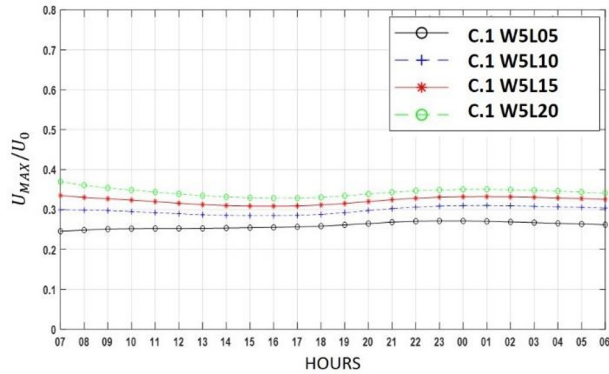


**Fig. 3.** Daily variation of the maximum nondimensional velocity  $U_{MAX}/U_0$  in the internal court of courtyard 1 versus time (hours of the day), for the different simulated courtyard dimensions (in the legend);  $U_0$  is the undisturbed wind velocity.

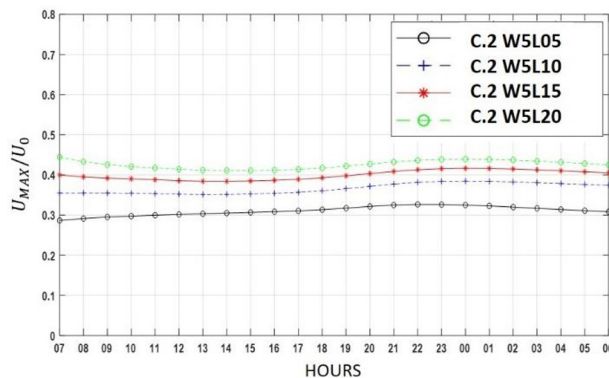


**Fig. 4.** Daily variation of the maximum nondimensional velocity  $U_{MAX}/U_0$  in the internal court of courtyard 2 versus time (hours of the day), for the different simulated courtyard dimensions (in the legend);  $U_0$  is the undisturbed wind velocity.

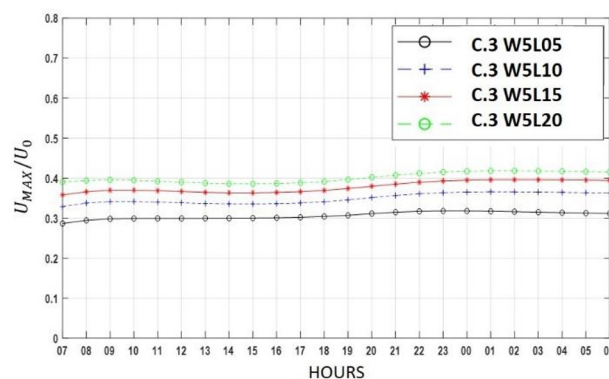


**Fig. 5.** Daily variation of the maximum nondimensional velocity  $U_{MAX}/U_0$  in the internal court of courtyard 3 versus time (hours of the day), for the different simulated courtyard dimensions (in the legend);  $U_0$  is the undisturbed wind velocity.

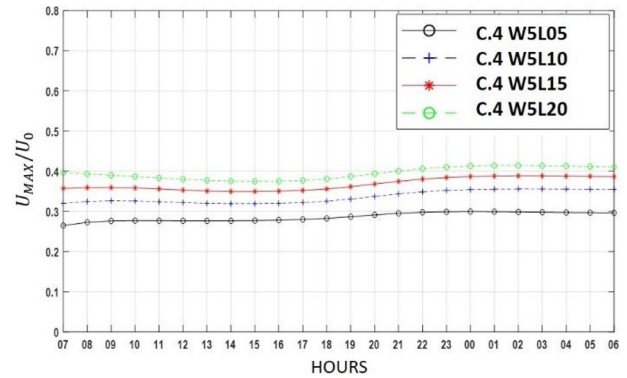


**Fig. 6.** Daily variation of the maximum nondimensional velocity  $U_{MAX}/U_0$  in the internal court of courtyard 4 versus time (hours of the day), for the different simulated courtyard dimensions (in the legend);  $U_0$  is the undisturbed wind velocity.

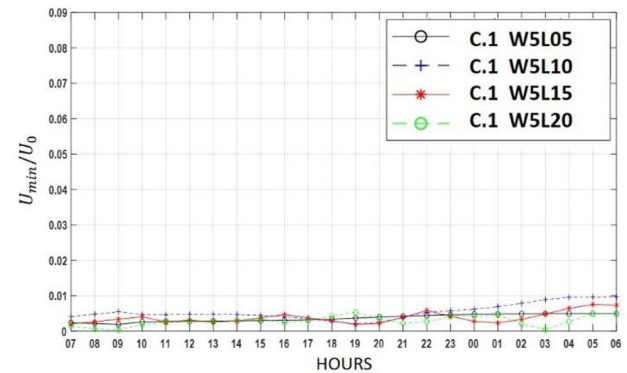


**Fig. 7.** Daily variation of the minimum nondimensional velocity  $U_{min}/U_0$  in the internal court of courtyard 1 versus time (hours of the day), for the different simulated courtyard dimensions (in the legend);  $U_0$  is the undisturbed wind velocity.

It is possible to see that the minimum velocity values inside the internal volume of C.1 are very similar for the different configurations, even if with some oscillations, and almost always lower than 1% of the undisturbed external velocity. The highest values are always found in the superior region of the internal courtyards' volume, while the lowest ones close to the pedestrian level, confirming the good mitigative features of the courtyard buildings.

In conclusion, the velocity variation imposed by the group of courtyard buildings when hit by a diagonal wind has a similar dependence on the internal courtyard length increase as in the case of perpendicular wind, investigated in Ferrari, 2022-a [43].

### 3.2 Pollutant concentration reduction

Fig. 8 shows a zoom on the group of courtyards of the horizontal field (measured at the pedestrian level, in this case 2m from the ground) of the non-dimensional pollutant concentration  $C/C_0$  (i.e., the pollutant concentration reduction, as  $C_0$  is the pollutant concentration at the chimneystack outlet, that is the maximum concentration in the domain). The concentration reduction values are showed in false colours, so that values close to the maximum are in pale

yellow and values close to the minimum (zero) are in dark blue. Moreover, as for the wind velocity, the white arrows represent the velocity direction and magnitude: the values are lower than for the wind velocity because here the values are measured closer to the ground.

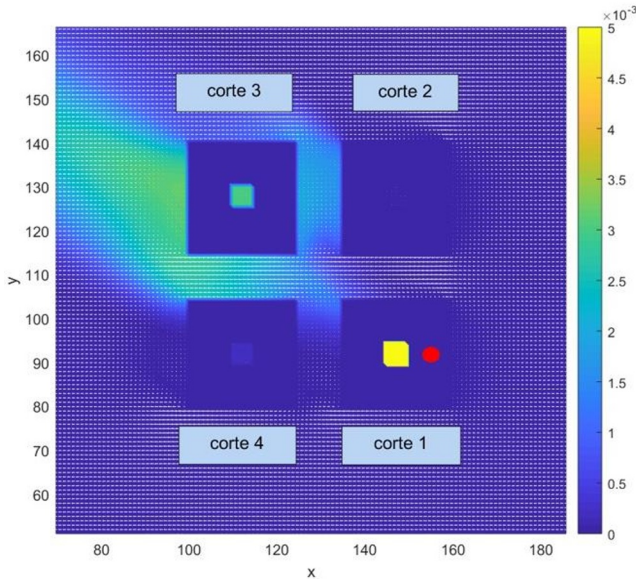


**Fig. 8.** Horizontal field of nondimensional pollutant concentration  $C/C_0$  at the pedestrian level (wind comes from East-South-East), for the configuration W5L05; the position of the pollutant source is highlighted in red.

As the wind comes from the East-South-East direction, it is visible that the pollutant, due to the air flow reattachment, enters into the internal courtyard C.1 space, but also into the C.3 and C.4, while the penetration into the C.2 is limited. Moreover, the wake of the pollutant along the wind direction is clearly visible downstream the C.3, as well as in the streets, in particular at the end of the S.1.

The effect of the courtyard dimensions on the concentration reduction, that the designer or the urban planner could use to reduce the interaction with a pollutant released from a chimneystack on the rooftop of a building in the urban environment, is shown on Fig. from 9 to 12 (for the internal space of the courtyards) and on Fig. from 13 to 15 (for the streets).

In particular, on Fig. from 9 to 12 (for, respectively, the courtyards from C.1 to C.4) the daily variation of the non-dimensional maximum pollutant concentration  $C_{MAX}/C_0$ , measured at the pedestrian level, is plotted for the four simulated configurations. On Fig. from 13 to 15,  $C_{MAX}/C_0$  inside the three streets (S.1, S.2 and S.3, respectively), measured at the pedestrian level, is plotted for the four simulated configurations. The values for the various cases W5L05, W5L10, W5L15 and W5L20, are shown with the same symbols employed above for the wind velocity. The minimum non-dimensional concentration inside the courtyards at pedestrian level is not shown, because it is always and everywhere almost zero.

First of all, all the Fig. from 9 to 12 shows a temporal dependence strongest than for the wind velocity, related to the different energy supplied by the sunlight at the different moment of the day, which makes variable the

turbulent stirring as well: for this reason, the concentration values are lower during the warmest hours of the day and higher during the coolest ones, phenomenon particularly visible in C.1 and C.3.

The highest values can be found in the C.1, the closest one to the chimneystack, highlighting that the design strategy, often employed in the engineering and architectural practice, stating that placing a chimneystack above the maximum height of the roof is enough to avoid the released pollutant to reach the pedestrian level, is not confirmed. As already visible from Fig. 8, the second highest values are found in C.3, followed by C.4, with the lowest values found in C.2, whose internal courtyard is almost out of the pollutant wake. It is interesting to note that the pollutant released from the rooftop of a building can harm the downstream buildings as well.

When focusing on the analysis of dependence of the internal courtyard dimensions on the pollutant concentration reduction, it is interesting to note that this is different for the various courtyards. In particular, in C.1 the smallest courtyard experiences the lowest concentrations, as the small dimensions close to the pollutant source tends to reduce the possibility for the pollutant to penetrate the internal volume, while the largest courtyards are interested of highest pollutant concentrations. The C.3 shows an inverse relation between pollutant concentration and internal courtyard dimensions: this could be related to what happens in C.1, as a larger pollutant quantity is trapped inside the first courtyards and, consequently, less pollutant can travel towards the downstream ones.

Fig. 13 shows that on S.1 the daily variation of  $C_{MAX}/C_0$  tends to be the same for all the simulated configurations, with a weak inverse dependence on the courtyard dimension. Fig. 14 and 15 show that the temporal dependence on S.2 and S.3 is similar, with highest values during the hottest hours of the day, that can be due a higher strength of the vortex's accumulation pollutant. The two streets show different dependences on the courtyard dimensions, with S.2 showing an increase in concentration as the courtyard dimensions increase, while S.3 shows a decrease in concentration as the courtyard dimensions increase.

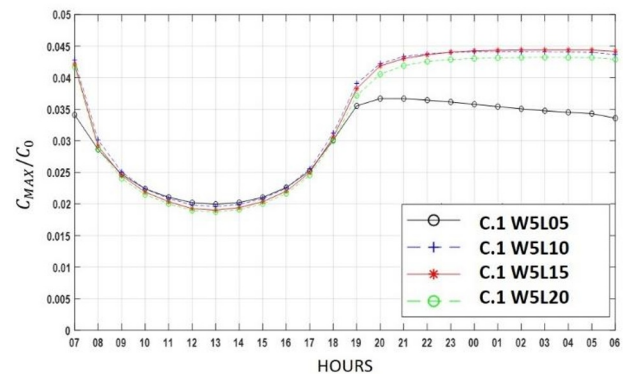


**Fig. 9.** Daily variation of the maximum nondimensional pollutant concentration  $C_{MAX}/C_0$  inside the courtyard 1 at the pedestrian level, for the different simulated courtyard dimensions (wind comes from East-South-East).

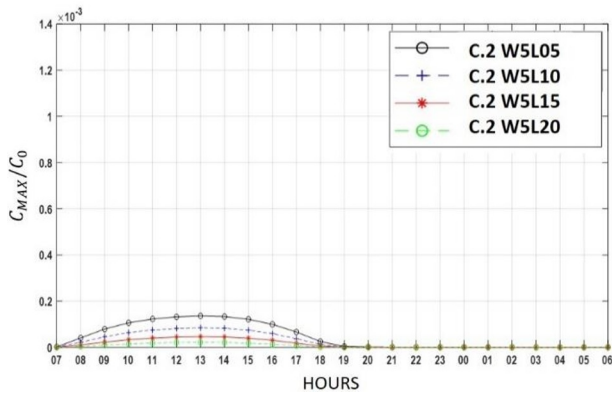


**Fig. 10.** Daily variation of the maximum nondimensional concentration pollutant concentration  $C_{MAX}/C_0$  inside the courtyard 2 at the pedestrian level, for the different simulated courtyard dimensions (wind comes from East-South-East).

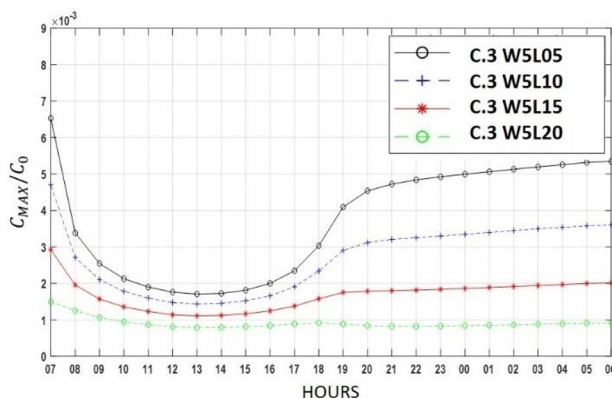


**Fig. 11.** Daily variation of the maximum nondimensional concentration pollutant concentration  $C_{MAX}/C_0$  inside the courtyard 3 at the pedestrian level, for the different simulated courtyard dimensions (wind comes from East-South-East).

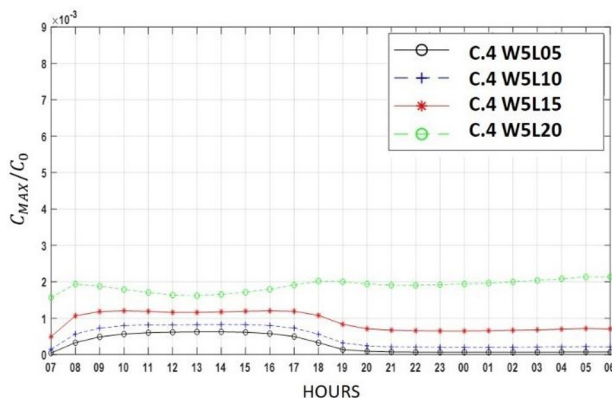


**Fig. 12.** Daily variation of the maximum nondimensional concentration pollutant concentration  $C_{MAX}/C_0$  inside the courtyard 4 at the pedestrian level, for the different simulated courtyard dimensions (wind comes from East-South-East).

In general, concentrations tend to be lower than in the case of the group of courtyard buildings when hit by a perpendicular wind, investigated in Ferrari, 2022-b [44].

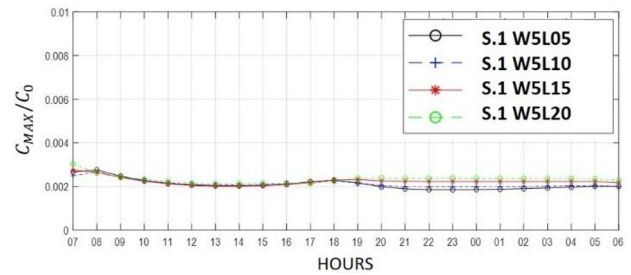


**Fig. 13.** Daily variation of the maximum nondimensional concentration pollutant concentration  $C_{MAX}/C_0$  inside the street 1 at the pedestrian level, for the different simulated courtyard dimensions (wind comes from East-South-East).

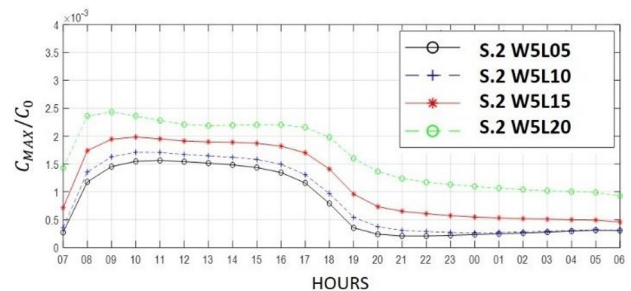


**Fig. 14.** Daily variation of the maximum nondimensional concentration pollutant concentration  $C_{MAX}/C_0$  inside the street 2 at the pedestrian level, for the different simulated courtyard dimensions (wind comes from East-South-East).

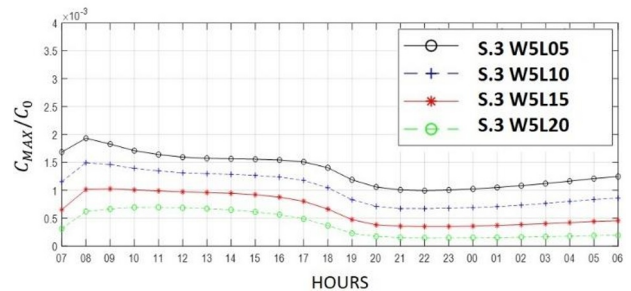


**Fig. 15.** Daily variation of the maximum nondimensional concentration pollutant concentration  $C_{MAX}/C_0$  inside the street 2 at the pedestrian level, for the different simulated courtyard dimensions (wind comes from East-South-East).

## 4 Conclusions

In this paper, we have investigated the capability of a group of courtyards, hit by a diagonal wind, to modulate the wind velocity variation and the pollutant dispersion in the internal courtyards and in the streets delimited by the buildings, through the variation of the internal courtyard length. The investigation has been carried out through a parametric study via numerical simulations with the ENVI-met<sup>®</sup> microclimate model.

In particular, the velocity values in the internal courtyard tends to be proportional to its volume in all the courtyards of the group, while the first courtyard encountered by the wind, is the one that experiences the highest wind velocity reduction, while the farther one is the one experiencing the highest ventilation. Moreover, the velocity variation is like the one measured when the group of courtyards is hit by a perpendicular wind. Consequently, the designer should increase the internal

courtyard dimensions if the target is to increase the ventilation, or vice-versa.

Regarding the pollutant dispersion, it has been shown that the pollutant enters the internal courtyard of the building with the chimneystack, but also in the courtyards downstream and in the streets, potentially harming the users of the urban environment. The closest courtyard to the chimneystack is the one that registers the highest pollutant concentrations, and to avoid this the designer should employ the smallest dimensions of the internal courtyard. Moreover, concentrations tend to be lower when the group of courtyards is hit by a diagonal wind than when it is hit by a perpendicular wind. This should be taken into account when planning the urban environment orientation to the prevalent winds, in presence of pollutant releases.

These results highlight the possibility to model the ventilation and pollutant dispersion in the built environment through the proper use of the buildings' proportions and location.

## References

- [1] S. Sharples e R. Bensalem, «Airflow in courtyard and atrium buildings in the urban environment: a wind tunnel study», *Sol. Energy*, vol. 70, fasc. 3, pp. 237–244, 2001, doi: 10.1016/S0038-092X(00)00092-X.
- [2] A. Gidlöf-Gunnarsson e E. Öhrström, «Attractive “Quiet” Courtyards: A Potential Modifier of Urban Residents’ Responses to Road Traffic Noise?», *Int. J. Environ. Res. Public Health*, vol. 7, fasc. 9, pp. 3359–3375, ago. 2010, doi: 10.3390/ijerph7093359.
- [3] V. Ok, E. Yasa, e M. Özgünler, «An Experimental Study of the Effects of Surface Openings on Air Flow Caused by Wind in Courtyard Buildings», *Archit. Sci. Rev.*, vol. 51, fasc. 3, pp. 263–268, set. 2008, doi: 10.3763/asre.2008.5131.
- [4] C. Ratti, D. Raydan, e K. Steemers, «Building form and environmental performance: archetypes, analysis and an arid climate», *Energy Build.*, vol. 35, fasc. 1, pp. 49–59, gen. 2003, doi: 10.1016/S0378-7788(02)00079-8.
- [5] Z. Zamani, S. Heidari, e P. Hanachi, «Reviewing the thermal and microclimatic function of courtyards», *Renew. Sustain. Energy Rev.*, vol. 93, pp. 580–595, ott. 2018, doi: 10.1016/j.rser.2018.05.055.
- [6] G. M. Chiri, M. Achenza, A. Cani, L. Neves, L. Tendas, e S. Ferrari, «The Microclimate Design Process in Current African Development: The UEM Campus in Maputo, Mozambique», *Energies*, vol. 13, fasc. 9, p. 2316, mag. 2020, doi: 10.3390/en13092316.
- [7] M. Santamouris, *Energy and climate in the urban built environment*. in BEST (Buildings Energy and Solar Technology). London: James & James, 2001.
- [8] P. De Pascali, *Città ed energia. La valenza energetica dell'organizzazione insediativa*. in Territorio governance sostenibilità. Saggi. Milano: Franco Angeli, 2008.
- [9] I. Eliasson, «The use of climate knowledge in urban planning», *Landsc. Urban Plan.*, vol. 48, fasc. 1–2, pp. 31–44, apr. 2000, doi: 10.1016/S0169-2046(00)00034-7.
- [10] World Health Organization, *WHO global air quality guidelines: particulate matter (PM2.5 and PM10), ozone, nitrogen dioxide, sulfur dioxide and carbon monoxide. Executive summary*. United nations, 2021.
- [11] M. Kurppa, A. Hellsten, M. Auvinen, S. Raasch, T. Vesala, e L. Järvi, «Ventilation and Air Quality in City Blocks Using Large-Eddy Simulation—Urban Planning Perspective», *Atmosphere*, vol. 9, fasc. 2, p. 65, feb. 2018, doi: 10.3390/atmos9020065.
- [12] M. G. Badas, M. Garau, A. Seoni, S. Ferrari, e G. Querzoli, «Impact of rooftop stack configuration on 2D street canyon air quality», *J. Phys. Conf. Ser.*, vol. 1110, p. 012003, nov. 2018, doi: 10.1088/1742-6596/1110/1/012003.
- [13] S. Ferrari, M. G. Badas, M. Garau, L. Salvadori, A. Seoni, e G. Querzoli, «On The Effect Of The Shape Of Buildings And Chimneystack On Ventilation And Pollutant Dispersion», *EPJ Web Conf.*, vol. 213, p. 02017, 2019, doi: 10.1051/epjconf/201921302017.
- [14] Y. Tamura, *Advanced environmental wind engineering*. New York, NY: Springer Berlin Heidelberg, 2016.
- [15] D. Lai, W. Liu, T. Gan, K. Liu, e Q. Chen, «A review of mitigating strategies to improve the thermal environment and thermal comfort in urban outdoor spaces», *Sci. Total Environ.*, vol. 661, pp. 337–353, apr. 2019, doi: 10.1016/j.scitotenv.2019.01.062.
- [16] S. Ferrari, R. Rossi, e A. Di Bernardino, «A Review of Laboratory and Numerical Techniques to Simulate Turbulent Flows», *Energies*, vol. 15, fasc. 20, p. 7580, ott. 2022, doi: 10.3390/en15207580.
- [17] A. D. Bernardino, P. Monti, G. Leuzzi, F. Sammartino, e S. Ferrari, «Experimental investigation of turbulence and dispersion around an isolated cubic building», in *HARMO 2017 - 18th International Conference on Harmonisation within Atmospheric Dispersion Modelling for Regulatory Purposes, Proceedings*, vol. 2017, Hungarian Meteorological Service, 2017, pp. 460–464.
- [18] S. Ferrari e G. Querzoli, «Laboratory experiments on the interaction between inclined negatively buoyant jets and regular waves», *EPJ Web Conf.*, vol. 92, p. 02018, 2015, doi: 10.1051/epjconf/20159202018.
- [19] S. Ferrari, M. G. Badas, M. Garau, A. Seoni, e G. Querzoli, «The air quality in narrow two-dimensional urban canyons with pitched and flat roof buildings», *Int. J. Environ. Pollut.*, vol. 62, fasc. 2/3/4, p. 22, 2017, doi: 0957-4352.
- [20] M. Garau, M. G. Badas, S. Ferrari, A. Seoni, e G. Querzoli, «Turbulence and Air Exchange in a



- Two-Dimensional Urban Street Canyon Between Gable Roof Buildings», *Bound.-Layer Meteorol.*, vol. 167, fasc. 1, pp. 123–143, apr. 2018, doi: 10.1007/s10546-017-0324-4.
- [21] M. G. Badas, S. Ferrari, M. Garau, A. Seoni, e G. Querzoli, «On the Flow Past an Array of Two-Dimensional Street Canyons Between Slender Buildings», *Bound.-Layer Meteorol.*, vol. 174, fasc. 2, pp. 251–273, feb. 2020, doi: 10.1007/s10546-019-00484-x.
- [22] S. Ferrari, «Image analysis techniques for the study of turbulent flows», *EPJ Web Conf.*, vol. 143, p. 01001, 2017, doi: 10.1051/epjconf/201714301001.
- [23] M. G. Badas, S. Ferrari, M. Garau, e G. Querzoli, «On the effect of gable roof on natural ventilation in two-dimensional urban canyons», *J. Wind Eng. Ind. Aerodyn.*, vol. 162, pp. 24–34, mar. 2017, doi: 10.1016/j.jweia.2017.01.006.
- [24] M. Garau, M. G. Badas, S. Ferrari, A. Seoni, e G. Querzoli, «Air Exchange in urban canyons with variable building width: a numerical LES approach», *Int. J. Environ. Pollut.*, vol. 65, fasc. 1–3, pp. 103–124, 2019, doi: 10.1504/IJEP.2019.101836.
- [25] H. Sun, C. Jimenez-Bescos, M. Mohammadi, F. Zhong, e J. K. Calautit, «Numerical Investigation of the Influence of Vegetation on the Aero-Thermal Performance of Buildings with Courtyards in Hot Climates», *Energies*, vol. 14, fasc. 17, p. 5388, ago. 2021, doi: 10.3390/en14175388.
- [26] D. Cui *et al.*, «Effects of building layouts and envelope features on wind flow and pollutant exposure in height-asymmetric street canyons», *Build. Environ.*, vol. 205, p. 108177, nov. 2021, doi: 10.1016/j.buildenv.2021.108177.
- [27] M. G. Badas, M. Garau, G. Querzoli, L. Salvadori, e S. Ferrari, «Urban areas parametrization for CFD simulation and cities air quality analysis», *Int. J. Environ. Pollut.*, vol. in press, 2019, doi: 10.1504/IJEP.2020.10022368.
- [28] L. Salvadori, M. G. Badas, A. Di Bernardino, G. Querzoli, e S. Ferrari, «A Street Graph-Based Morphometric Characterization of Two Large Urban Areas», *Sustainability*, vol. 13, fasc. 3, p. 1025, gen. 2021, doi: 10.3390/su13031025.
- [29] L. Salvadori, A. Di Bernardino, G. Querzoli, e S. Ferrari, «A Novel Automatic Method for the Urban Canyon Parametrization Needed by Turbulence Numerical Simulations for Wind Energy Potential Assessment», *Energies*, vol. 14, fasc. 16, p. 4969, ago. 2021, doi: 10.3390/en14164969.
- [30] R. Ernest e B. Ford, «The role of multiple-courtyards in the promotion of convective cooling», *Archit. Sci. Rev.*, vol. 55, fasc. 4, pp. 241–249, nov. 2012, doi: 10.1080/00038628.2012.723400.
- [31] X. Xu, F. Luo, W. Wang, T. Hong, e X. Fu, «Performance-Based Evaluation of Courtyard Design in China’s Cold-Winter Hot-Summer Climate Regions», *Sustainability*, vol. 10, fasc. 11, p. 3950, ott. 2018, doi: 10.3390/su10113950.
- [32] J. Rodríguez-Algeciras, A. Tablada, M. Chaos-Yeras, G. De la Paz, e A. Matzarakis, «Influence of aspect ratio and orientation on large courtyard thermal conditions in the historical centre of Camagüey-Cuba», *Renew. Energy*, vol. 125, pp. 840–856, set. 2018, doi: 10.1016/j.renene.2018.01.082.
- [33] C. Rivera-Gómez, E. Diz-Mellado, C. Galán-Marín, e V. López-Cabeza, «Tempering potential-based evaluation of the courtyard microclimate as a combined function of aspect ratio and outdoor temperature», *Sustain. Cities Soc.*, vol. 51, p. 101740, nov. 2019, doi: 10.1016/j.scs.2019.101740.
- [34] X. Ma, J. Zhao, e P. Guo, «The urban computing on the distribution of inhalable particulate matters to Smart City-based residential groups», *Concurr. Comput. Pract. Exp.*, vol. 31, fasc. 9, p. e4803, mag. 2019, doi: 10.1002/cpe.4803.
- [35] K. Piedra, W. Bustamante, e C. Schmitt, «Living and Comfort Conditions in Heritage Housing: The Inner Courtyard as a Uniting Element in the Cités of Santiago Poniente», *IOP Conf. Ser. Earth Environ. Sci.*, vol. 503, p. 012010, giu. 2020, doi: 10.1088/1755-1315/503/1/012010.
- [36] E. Diz-Mellado, V. P. López-Cabeza, C. Rivera-Gómez, C. Galán-Marín, J. Rojas-Fernández, e M. Nikolopoulou, «Extending the adaptive thermal comfort models for courtyards», *Build. Environ.*, vol. 203, p. 108094, ott. 2021, doi: 10.1016/j.buildenv.2021.108094.
- [37] Z. Du, W. Guo, W. Li, e X. Gao, «A Study on the Optimization of Wind Environment of Existing Villa Buildings in Lingnan Area: A Case Study of Jiangmen’s “Yunshan Poetic” Moon Island Houses», *Buildings*, vol. 12, fasc. 9, p. 1304, ago. 2022, doi: 10.3390/buildings12091304.
- [38] I. J. A. Callejas e E. Krüger, «Microclimate and thermal perception in courtyards located in a tropical savannah climate», *Int. J. Biometeorol.*, vol. 66, fasc. 9, pp. 1877–1890, ago. 2022, doi: 10.1007/s00484-022-02329-8.
- [39] M. Taleghani, M. Tenpierik, e A. van den Dobbelsteen, «Energy performance and thermal comfort of courtyard/atrium dwellings in the Netherlands in the light of climate change», *Renew. Energy*, vol. 63, pp. 486–497, mar. 2014, doi: 10.1016/j.renene.2013.09.028.
- [40] L. Martinelli e A. Matzarakis, «Influence of height/width proportions on the thermal comfort of courtyard typology for Italian climate zones», *Sustain. Cities Soc.*, vol. 29, pp. 97–106, feb. 2017, doi: 10.1016/j.scs.2016.12.004.
- [41] X. Ying, Y. Wang, W. Li, Z. Liu, e G. Ding, «Group Layout Pattern and Outdoor Wind Environment of Enclosed Office Buildings in Hangzhou», *Energies*, vol. 13, fasc. 2, p. 406, gen. 2020, doi: 10.3390/en13020406.
- [42] I. J. Apolonio Callejas, L. Cleonice Durante, E. Diz-Mellado, e C. Galán-Marín, «Thermal

- Sensation in Courtyards: Potentialities as a Passive Strategy in Tropical Climates», *Sustainability*, vol. 12, fasc. 15, p. 6135, lug. 2020, doi: 10.3390/su12156135.
- [43] S. Ferrari, «Ventilation in a group of courtyard buildings», *EPJ Web Conf.*, vol. 264, p. 01014, 2022, doi: 10.1051/epjconf/202226401014.
- [44] S. Ferrari, «Pollutant dispersion in a group of courtyard buildings», *EPJ Web Conf.*, vol. 264, p. 01013, 2022, doi: 10.1051/epjconf/202226401013.
- [45] M. Bruse e H. Fleer, «Simulating surface-plant-air interactions inside urban environments with a three dimensional numerical model», *Environ. Model. Softw.*, vol. 13, fasc. 3–4, pp. 373–384, 1998, doi: 10.1016/S1364-8152(98)00042-5.
- [46] B. Blocken, «Computational Fluid Dynamics for urban physics: Importance, scales, possibilities, limitations and ten tips and tricks towards accurate and reliable simulations», *Build. Environ.*, vol. 91, pp. 219–245, set. 2015, doi: 10.1016/j.buildenv.2015.02.015.
- [47] M. Mosteiro-Romero e D. Maiullari, «An Integrated Microclimate-Energy Demand Simulation Method for the Assessment of Urban Districts», *Front. Built Environ.*, vol. 6, 2020.
- [48] F. Salata, I. Golasi, R. de Lieto Vollaro, e A. de Lieto Vollaro, «Urban microclimate and outdoor thermal comfort. A proper procedure to fit ENVI-met simulation outputs to experimental data», *Sustain. Cities Soc.*, vol. 26, pp. 318–343, ott. 2016, doi: 10.1016/j.scs.2016.07.005.
- [49] A. Forouzandeh, «Numerical modeling validation for the microclimate thermal condition of semi-closed courtyard spaces between buildings», *Sustain. Cities Soc.*, vol. 36, pp. 327–345, gen. 2018, doi: 10.1016/j.scs.2017.07.025.
- [50] A. Forouzandeh, «Prediction of surface temperature of building surrounding envelopes using holistic microclimate ENVI-met model», *Sustain. Cities Soc.*, vol. 70, p. 102878, lug. 2021, doi: 10.1016/j.scs.2021.102878.
- [51] D. (Jian) Sun, S. Wu, S. Shen, e T. Xu, «Simulation and assessment of traffic pollutant dispersion at an urban signalized intersection using multiple platforms», *Atmospheric Pollut. Res.*, vol. 12, fasc. 7, p. 101087, lug. 2021, doi: 10.1016/j.apr.2021.101087.
- [52] M. Viecco, H. Jorquera, A. Sharma, W. Bustamante, H. J. S. Fernando, e S. Vera, «Green roofs and green walls layouts for improved urban air quality by mitigating particulate matter», *Build. Environ.*, vol. 204, p. 108120, ott. 2021, doi: 10.1016/j.buildenv.2021.108120.
- [53] J. Wu, K. Luo, Y. Wang, e Z. Wang, «Urban road greenbelt configuration: The perspective of PM2.5 removal and air quality regulation», *Environ. Int.*, vol. 157, p. 106786, dic. 2021, doi: 10.1016/j.envint.2021.106786.
- [54] L. Jing e Y. Liang, «The impact of tree clusters on air circulation and pollutant diffusion-urban micro scale environmental simulation based on ENVI-met», *IOP Conf. Ser. Earth Environ. Sci.*, vol. 657, p. 012008, feb. 2021, doi: 10.1088/1755-1315/657/1/012008.
- [55] M. Karimian Shamsabadi, M. Yeganeh, e E. Pourmahabadian, «Urban buildings configuration and pollutant dispersion of PM 2.5 particulate to enhance air quality», *Front. Sustain. Food Syst.*, vol. 6, p. 898549, set. 2022, doi: 10.3389/fsufs.2022.898549.
- [56] S. N. Kandelan, M. Yeganeh, S. Peyman, K. Panchabikesan, e U. Eicker, «Environmental study on greenery planning scenarios to improve the air quality in urban canyons», *Sustain. Cities Soc.*, vol. 83, p. 103993, ago. 2022, doi: 10.1016/j.scs.2022.103993.
- [57] Z. Peng, R. Debnath, R. Bardhan, e K. Steemers, «Machine learning-based evaluation of dynamic thermal-tempering performance and thermal diversity for 107 Cambridge courtyards», *Sustain. Cities Soc.*, vol. 88, p. 104275, gen. 2023, doi: 10.1016/j.scs.2022.104275.
- [58] K. Fabbri e V. Costanzo, «Drone-assisted infrared thermography for calibration of outdoor microclimate simulation models», *Sustain. Cities Soc.*, vol. 52, p. 101855, gen. 2020, doi: 10.1016/j.scs.2019.101855.
- [59] T. R. Oke, «Street design and urban canopy layer climate», *Energy Build.*, vol. 11, fasc. 1, pp. 103–113, mar. 1988, doi: 10.1016/0378-7788(88)90026-6.